Bioorganic & Medicinal Chemistry Letters 25 (2015) 690–694

Contents lists available at ScienceDirect

Bioorganic & Medicinal Chemistry Letters

journal homepage: www.elsevier.com/locate/bmcl

Further optimization of the M_5 NAM MLPCN probe ML375: Tactics and challenges

Haruto Kurata [b,c], Patrick R. Gentry [b,c], Masaya Kokubo [b,c], Hyekyung P. Cho [a,b,c], Thomas M. Bridges [a,b,c], Colleen M. Niswender [a,b,c], Frank W. Byers [a,b,c], Michael R. Wood [a,b,c], J. Scott Daniels [a,b,c], P. Jeffrey Conn [a,b,c], Craig W. Lindsley [a,b,c,d,*]

[a] *Department of Pharmacology, Vanderbilt University Medical Center, Nashville, TN 37232, USA*
[b] *Vanderbilt Center for Neuroscience Drug Discovery, Vanderbilt University Medical Center, Nashville, TN 37232, USA*
[c] *Vanderbilt Specialized Chemistry Center for Probe Development (MLPCN), Nashville, TN 37232, USA*
[d] *Department of Chemistry, Vanderbilt University, Nashville, TN 37232, USA*

ARTICLE INFO

Article history:
Received 27 October 2014
Revised 25 November 2014
Accepted 27 November 2014
Available online 13 December 2014

Keywords:
M_5
Muscarinic receptor
Negative allosteric modulator
Matrix library
Pharmacokinetics

ABSTRACT

This Letter describes the continued optimization of the MLPCN probe ML375, a highly selective M_5 negative allosteric modulator (NAM), through a combination of matrix libraries and iterative parallel synthesis. True to certain allosteric ligands, SAR was shallow, and the matrix library approach highlighted the challenges with M_5 NAM SAR within in this chemotype. Once again, enantiospecific activity was noted, and potency at rat and human M_5 were improved over ML375, along with slight enhancement in physiochemical properties, certain in vitro DMPK parameters and CNS distribution. Attempts to further enhance pharmacokinetics with deuterium incorporation afforded mixed results, but pretreatment with a *pan*-P450 inhibitor (1-aminobenzotriazole; ABT) provided increased plasma exposure.

Of the five muscarinic acetylcholine receptors (mAChR subtypes M_1–M_5), far less in known about the neurobiological roles of M_5 due both to limited CNS expression (<2% of all mAChR protein in rat brain and found exclusively in the ventral tegmental area [VTA] on dopamine transporter [DAT]-expressing neurons and in the substantia nigra pars compacta [SNc]) and the lack of highly selective, in vivo probe molecules.[1–10] Insight into the therapeutic potential of M_5 comes largely from genetic studies in M_5-KO mice, which exhibit reduced sensitivity to the rewarding effects of cocaine and opiates.[11–13] Recently, an association between an M_5 SNP and an addictive phenotype was observed in man, directly linking M_5 to drug abuse and reward.[14] To advance the M_5 research field, small molecule probes are required to recapitulate the genetic data.

Previously, we have reported on the development of several potent and selective M_5 positive allosteric modulator (PAM) chemotypes,[15–18] as well as the first highly M_5 selective orthosteric antagonist;[19] however, DMPK properties were generally poor and these efforts failed to produce in vivo probes. Last year we disclosed results from an M_5 functional high-throughput screen that provided 1-(4-flurobenzoyl)-9b-phenyl-2,3-dihydro-1*H*-imidazo-[2,1-*a*]isoindol-5(9b*H*)-one as an M_5 negative allosteric modulator (NAM) hit, **1** (Fig. 1).[20] A limited chemical optimization effort afforded ML375 (**2**), the first M_5-selective NAM with favorable CNS exposure (brain/plasma $K_p = 1.8$), moderate PK, high plasma protein binding (rat $f_u = 0.029$, human $f_u = 0.013$, rat brain $f_u = 0.003$) and enantiospecific activity (only the (*S*)-enantiomer of the 9b *p*-Cl phenyl was active).[20] Despite a major advance in the field, due to weak potency at rat M_5, coupled with high plasma protein and brain homogenate binding, ML375 lacked the requisite free drug exposure to serve as an in vivo tool compound.[20] In this Letter, we report on the continued optimization of our first-in-class M_5 NAM, and detail key tactics and noteworthy challenges en route to an M_5 NAM in vivo probe.

The synthesis of novel analogs of ML375 required a simple two-step synthesis involving condensation of ethylene diamine and an appropriately substituted 2-benzoylbenzoic acid **3** (or heteroaromatic/cyclo(hetero)alkyl congener) to provide **4**, followed by a subsequent acylation reaction (Scheme 1) to deliver ML375 analogs **5**–**7**.[20,21] However, we quickly exhausted the commercial analogs of **3**. Fortunately, we were able to employ three synthetic routes to access key intermediates **3** with either diverse substituents or encompassing heterocycles.

* Corresponding author.
E-mail address: craig.lindsley@vanderbilt.edu (C.W. Lindsley).

http://dx.doi.org/10.1016/j.bmcl.2014.11.082
0960-894X/

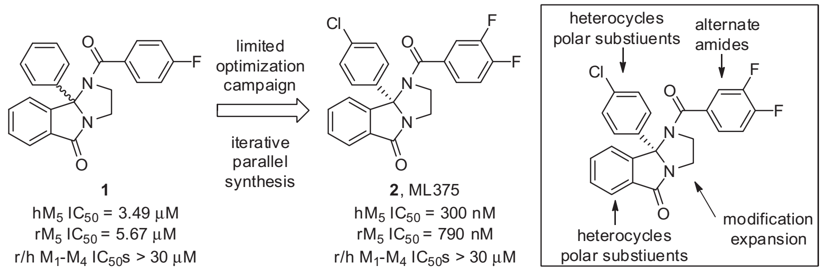

Figure 1. Structures and mAChR activities of M_5 NAM HTS hit **1**, and the optimized MLPCN probe ML375 (**2**). Inset, optimization plan for ML375 to improve rat potency and physiochemical/disposition properties. Potency values determined via a functional calcium mobilization assay in the presence of a fixed acetylcholine EC_{80} in recombinant cells.[20]

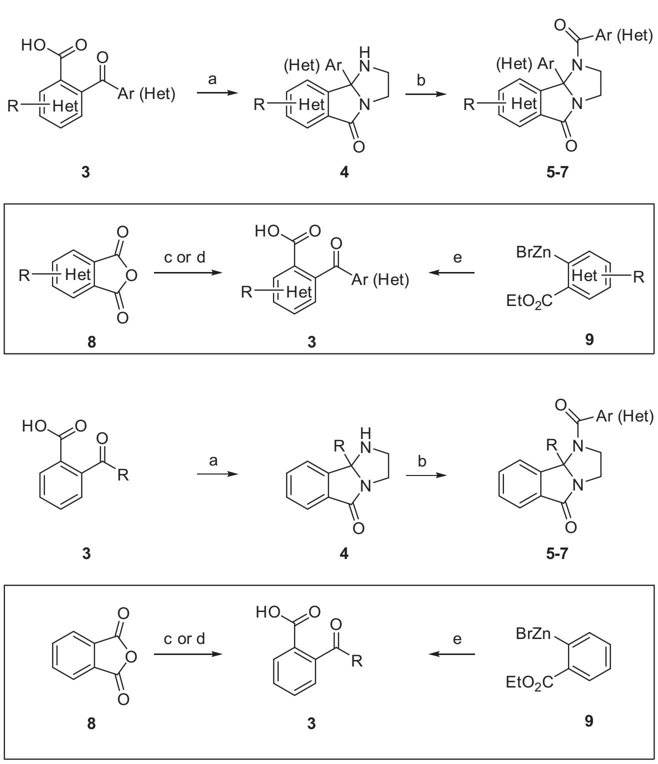

Scheme 1. Reagents and conditions: (a) ethylene diamine, *p*-TSA, toluene (+1,4-dioxane), reflux, Dean–Stark trap, or microwave irradiation 130-150 °C 4–77%; (b) Ar(Het)COCl, CH_2Cl_2, DIPEA, 16–91%; (c) RMgX, THF, −65 °C to 0 °C or rt, 8–68%; (d) R-H, $AlCl_3$, $PhNO_2$, rt, 41–88%; (e) (i) RCOCl, cat. Ni(acac)$_2$, THF, rt, (ii) aq NaOH, EtOH/THF, rt, 31–55%.

In the first round of library synthesis, we held the *p*-Cl 9b phenyl moiety of ML375 constant, and scanned alternate amides within a racemic core to provide analogs **5**. Here, (Table 1) we found that heterocycles were generally not tolerated (**5i–l**) in the context of the *p*-Cl 9b phenyl core, but two amide congeners, the 4-isoproxyphenyl (**5f**) and the 3,4,5-trifluorophenyl (**5g**), displayed submicromolar human M_5 activity (hM_5 IC_{50}s of 790 nM and 610 nM, respectively), yet were less potent than racemic ML375 (**5a**, hM_5 IC_{50} = 480 nM). Within a conserved series of ethers, hM_5 potency, for example, M_5 IC_{50}s, was enhanced as steric bulk increased—OMe (**5d**) < OEt (**5e**) < O*i*-Pr (**5f**). Despite the lower hM_5 potency, **5d** displayed a moderate improvement in *c*log*P* relative to **5a** (4.6 vs 5.2), so we elected to evaluate how diminished lipophilicity would impact plasma protein binding. While racemic **5a** displayed high plasma protein binding (rat f_u = 0.031, human f_u = 0.015), binding of **5f** was slightly decreased (rat f_u = 0.037, human f_u = 0.027). These findings then led us to pursue second generation libraries where we aimed to incorporate polar, basic and sp^3-hybridized ring systems into the 9b position, while holding the 3,4-difluorobenzoyl moiety constant, to assess if we could improve both physiochemical properties as well as hM_5 potency.

Following Scheme 1, analogs **6** were rapidly prepared and screened against hM_5 (Table 2). Once again, SAR was shallow, with all sp^3-based systems, as well as heterocycles, devoid of hM_5 activity. A similar pattern emerged for ethers between analog series **5** and **6**, with **6c**, the 4-OMe phenyl analog, superior potency (hM_5 IC_{50} = 1.3 μM), but insufficient to advance as an in vivo probe. As before, **6c** possessed a lower *c*log*P* (4.21), which translated into improved plasma free fraction (rat f_u = 0.064, human f_u = 0.037). Interestingly, the addition of more sp^3-character, in the form of the cyclohexyl congener **6e**, led to a higher *c*log*P* (5.2) and diminished free fraction (rat f_u = 0.016, human f_u = 0.008). In parallel, we replaced the phenyl ring at the 9b position with the three regioisomeric pyridines, and all were not tolerated (hM_5 IC_{50} >5 μM), as were ring expansions and substitutions of the 1*H*-imidazo[2, 1-*a*]isoindol-5(9b*H*)-one core.

At a loss for a rational, singleton approach to build-in hM_5 potency and improved physiochemical properties, we elected to pursue a 3 × 9 matrix library of analogs **7** to systematically evaluate all the possible combinations of monomers that showed either hM_5 potency enhancement or improved physiochemical properties (Table 3).[22,23] While we have generated, on numerous occasions, robust, tractable SAR within GPCR allosteric ligand chemotypes, we have also reported on numerous accounts of chemotypes that possess shallow or flat SAR,[8–11,24] and this matrix library is an example of the latter. Here, the clear stand-out was racemic **7B-6** (also referred to as VU0652483, hM_5 IC_{50} = 517 nM, pIC_{50} = 6.29 ± 0.02), possessing a 3,4,5-trifluorobenzoyl amide and a 3-methyl-4-methoxy phenyl moiety in the 9b position. Due to the increased hM_5 potency, we evaluated VU0652483 potency at rat M_5 and found submicromolar activity (rat M_5 IC_{50} = 963 nM, pIC_{50} = 6.02 ± 0.04) as well. As all of the activity of ML375 resided in the (*S*)-enantiomer, we resolved the enantiomers of VU0652483 via chiral SFC to afford (*S*)-**7B-6** (VU6000181) and (*R*)-**7B-6** (VU6000180); here again, the (*R*)-enantiomer was inactive (Fig. 2) and the (*S*)-enantiomer, VU6000181, possessed all of the M_5 activity (hM_5 IC_{50} = 264 nM, pIC_{50} = 6.58 ± 0.03, rat M_5 IC_{50} = 516 nM, pIC_{50} = 6.29 ± 0.05), thus representing the most potent M_5 NAM reported to date and maintaining selectivity versus M_1–M_4 (IC_{50}s >30 μM).[20] Moreover, the *c*log*P* for VU6000181 (4.6) was improved over ML375 (5.2), and this once again translated into a slight improvement over ML375 (rat f_u = 0.031, human f_u = 0.013, rat brain f_u = 0.006). In addition, VU6000181 was highly centrally penetrant (brain/plasma K_p = 2.7 at 0.25 h post-administration), yet a high clearance compound in vitro (rat hepatic microsome CL_{INT} = 332 mL/min/kg, predicted CL_{HEP} = 57.8 mL/min/kg and human hepatic microsome CL_{INT} = 359 mL/min/kg, predicted CL_{HEP} = 19.8 mL/min/kg) and in vivo (rat CL_p = 80 mL/min/kg, $t_{1/2}$ = 65 min, V_{ss} = 4.9 L/kg). The PK profile of VU6000181 rendered it unsuitable as an in vivo probe.

Table 1
Structures and activities of analogs **5**

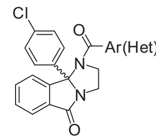

5

Entry	Ar (Het)	hM_5 IC_{50} (μM)	hM_5 pIC_{50}[a]	Entry	Ar (Het)	hM_5 IC_{50} (μM)	hM_5 pIC_{50}[a]
5a	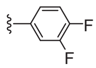	0.48	6.32 ± 0.03	**5g**	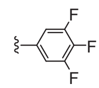	0.61	6.21 ± 0.02
5b	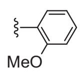	>10	>5	**5h**	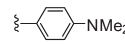	>10	>5
5c	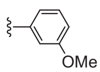	6.6	5.18 ± 0.16	**5i**	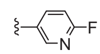	>10	>5
5d	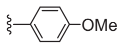	1.8	5.74 ± 0.08	**5j**	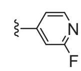	5.8	5.23 ± 0.09
5e	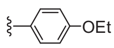	0.85	6.07 ± 0.05	**5k**	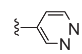	>10	>5
5f	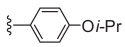	0.79	6.10 ± 0.03	**5l**	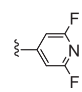	>10	>5

[a] hM_5 pIC_{50} reported as average ± SEM from our calcium mobilization assay; $n = 3$.

Table 2
Structures and activities of analogs **6**

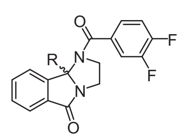

6

Entry	R	hM_5 IC_{50} (μM)	hM_5 pIC_{50}[a]	Entry	R	hM_5 IC_{50} (μM)	hM_5 pIC_{50}[a]
6a	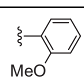	5.5	5.25 ± 0.07	**6g**	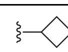	>10	>5
6b	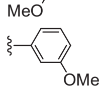	1.6	5.79 ± 0.04	**6h**	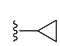	>10	>5
6c	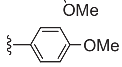	1.3	5.88 ± 0.01	**6i**	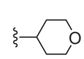	>10	>5
6d	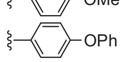	>10	>5	**6j**	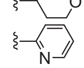	>10	>5
6e	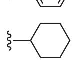	2.1	5.67 ± 0.05	**6k**	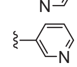	>10	>5
6f	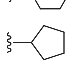	2.4	5.61 ± 0.06	**6l**	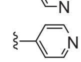	>10	>5

[a] hM_5 pIC_{50} reported as average ± SEM from our calcium mobilization assay; $n = 3$.

Previously, we productively utilized deuterium incorporation to overcome high clearance coupled with flat SAR in a series of $mGlu_3$ NAMs,[25] reducing rat in vitro and in vivo clearance by ~50% and affording an in vivo probe. Replacing the OCH_3 moiety of VU6000181 with a OCD_3 moiety (**10**, VU6001005) did in fact reduce human in vitro intrinsic clearance ~5-fold (human CL_{INT} = 72.9 mL/min/kg) but provided negligible improvement to rat intrinsic clearance, and thus, was not a productive path towards an in vivo tool compound (Fig. 3).

Finally, we performed an in vivo PK study by predosing rats with the *pan*-P450 inhibitor 1-aminobenzotriazole (ABT) in an attempt to potentially achieve therapeutically relevant drug levels and provide target validation for M_5 NAMs.[26] In this instance, we first pre-treated rats with an oral vehicle (10% tween 80 in 0.5% MC in water), followed 1.5 h later by VU6000181 at 10 mg/kg, po in 30% HPBCD in water (10 mg/mL). This control protocol revealed a VU6000181 mean residence time (MRT) of 6.5 h, a T_{max} of 2.8 h, an AUC_{0-inf} of 3660 (h ng/mL) and low oral bioavailability (%F = 2.0). Pre-treatment of rats with a 56.6 mg/kg dose of ABT PO (10% Tween 80 in 0.5% MC in water), followed 1.5 h later by VU6000181 at 10 mg/kg, PO in 30% HPBCD in water (10 mg/mL), provided a ~5-fold increase in exposure (AUC_{0-inf} of 17,700 (h ng/mL), %F = 9.5) relative to that in the vehicle pre-treated animals (Fig. 4). In addition, ABT pre-treatment afforded a ~3-fold

Table 3
Structures and activities of matrix library analogs **7**

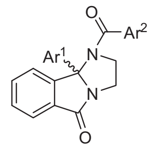

7

Entry	Ar2 A 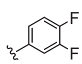 hM5 IC50[a] (μM)	Ar2 B 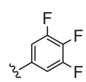 hM5 IC50[a] (μM)	Ar2 C 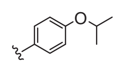 hM5 IC50[a] (μM)	Ar1
1	3.2	>30	4.1	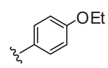
2	>30	2.4	1.9	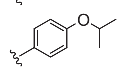
3	1.3	1.0	1.1	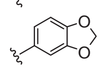
4	3.3	>30	3.2	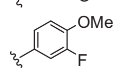
5	5.5	1.4	3.3	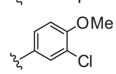
6	1.2	0.51	1.3	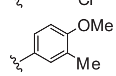
7	2.7	0.7	1.3	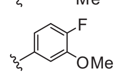
8	2.0	1.6	6.4	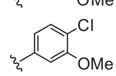
9	1.3	0.9	2.2	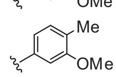

[a] hM_5 IC_{50} data, $n = 1$; hM_5 IC_{50} for **7B-6**, $n = 6$, $pIC_{50} = 6.29 \pm 0.02$.

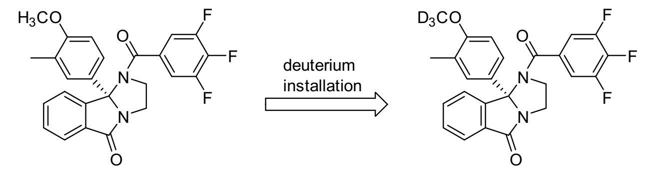

(*S*)-**7B-6**, VU6000181
human CL_{INT} = 359 mL/min/kg
human CL_{HEP} = 19.8 mL/min/kg

rat CL_{INT} = 332 mL/min/kg
rat CL_{HEP} = 57.8 mL/min/kg

8, VU6001005
human CL_{INT} = 72.9 mL/min/kg
human CL_{HEP} = 16.3 mL/min/kg

rat CL_{INT} = 275 mL/min/kg
rat CL_{HEP} = 55.8 mL/min/kg

Figure 3. The impact of deuterium incorporation into VU6000181 on human, but not rat, intrinsic clearance determined in hepatic microsomes fortified with NADPH (values represent means from one independent determination performed in triplicate).

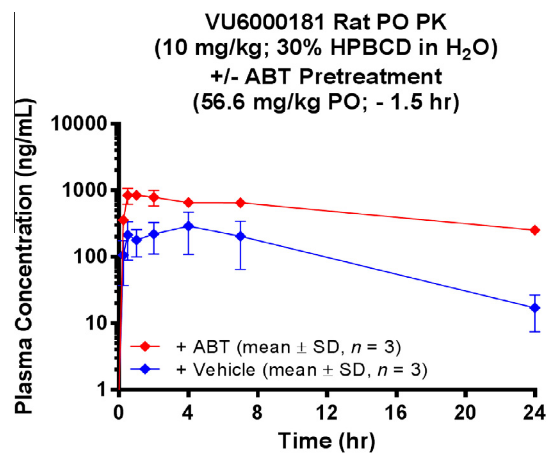

Figure 4. Oral plasma pharmacokinetics of VU6000181 in the absence (blue) or presence (red) of ABT pre-treatment in rats (male, Sprague-Dawley). ABT pre-treatment improved exposure ~5-fold and maximum concentrations ~3-fold.

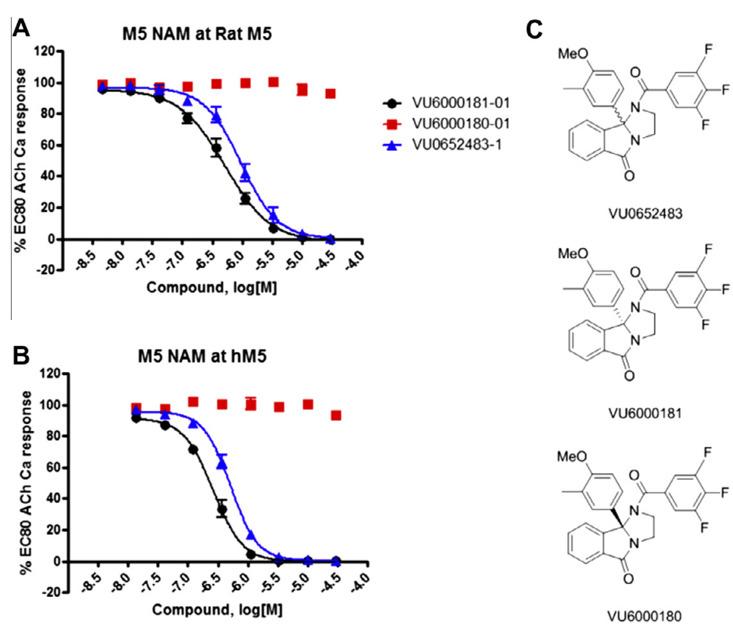

Figure 2. Structures and M_5 functional assay concentration–response-curves (CRCs) obtained in the presence of a fixed acetylcholine EC_{80} in recombinant cells. (A) rat M_5 CRCs of racemic VU0652483, the active (*S*)-enantiomer, VU6000181 and the inactive (*R*)-enantiomer, VU6000180; (B) human M_5 CRCs of racemic VU0652483, the active (*S*)-enantiomer, VU6000181 and the inactive (*R*)-enantiomer, VU6000180; (C) structures of VU0652483, VU6000181, VU6000180.

increase in C_{max} (plasma = 2.0 μM, ~62 nM unbound) and, based on the a brain/plasma K_p (2.7), projected C_{max} levels in brain in the presence of ABT would be ~5.4 μM (~32 nM unbound). Thus, ABT pretreatment may serve as a viable strategy to increase levels of VU6000181 for future fMRI and addiction studies to test selective M_5 inhibition hypotheses.

In summary, we reported on the continued optimization of the MLPCN probe ML375, a highly selective M_5 NAM, through a combination of matrix libraries and iterative parallel synthesis. While SAR can be highly tractable for certain allosteric ligands, this chemotype was a clear example of 'flat' or 'shallow' SAR, wherein an matrix library was critical in identifying a productive lead compound, VU6000181, with improved activity at rat M_5 and disposition relative to ML375. Attempts to improve PK by deuterium incorporation substantially impacted only human in vitro CL_{INT}, but ABT pre-treatment significantly increased exposure in rats, potentially affording a strategy to achieve target validation for selective M_5 inhibition. Efforts continue, and work is in progress to pharmacologically probe M_5 neurobiology and therapeutic potential with small molecules.

Acknowledgments

Vanderbilt is a member of the MLPCN and houses the Vanderbilt Specialized Chemistry Center for Accelerated Probe Development. This work was supported by the NIH/MLPCN Grant U54 MH084659 (C.W.L.), the Vanderbilt Department of Pharmacology and William K. Warren, Jr. who funded the William K. Warren, Jr. Chair in Medicine (to C.W.L.).

References and notes

1. Smythies, J. *Int. Rev. Neurobiol.* **2005**, *64*, 1.
2. Wess, J.; Eglen, R. M.; Gautam, D. *Nat. Rev. Drug Discov.* **2007**, *6*, 721.
3. Langmead, C. J.; Watson, J.; Reavill, C. *Pharmacol. Ther.* **2008**, *117*, 232.
4. Denker, D.; Thomsen, M.; Wortwein, G.; Weikop, G.; Cui, Y.; Jeon, J.; Wess, J.; Fink-Jensen, A. *ACS Chem. Neurosci.* **2012**, *3*, 80.
5. Caulfield, M. P.; Birdsall, N. J. M. *Pharmacol. Rev.* **1998**, *50*, 279.
6. Weiner, D. M.; Levey, A. I.; Brann, M. R. *Proc. Natl. Acad. Sci. U.S.A.* **1990**, *87*, 7050.
7. Yasuda, R. P.; Ciesla, W.; Flores, L. R.; Wall, S. J.; Li, M.; Satkus, S. A.; Weisstein, J. S.; Spagnola, B. V.; Wolfe, B. B. *Mol. Pharmacol.* **1993**, *43*, 149.
8. Melancon, B. J.; Hopkins, C. R.; Wood, M. R.; Emmitte, K. A.; Niswender, C. M.; Christopoulos, A.; Conn, P. J.; Lindsley, C. W. *J. Med. Chem.* **2012**, *55*, 1445.
9. Conn, P. J.; Jones, C.; Lindsley, C. W. *Trends Pharm. Sci.* **2009**, *30*, 148.
10. Lindsley, C. W. *J. Med. Chem.* **2014**, *57*, 7485.
11. Basile, A. S.; Fedorova, I.; Zapata, A.; Liu, X.; Shippenberg, T.; Duttaroy, A.; Yamada, M.; Wess, J. *Proc. Natl. Acad. Sci. U.S.A.* **2002**, *99*, 11452.
12. Fink-Jensen, A.; Fedorova, I.; Wörtwein, G.; Woldbye, D. P.; Rasmussen, T.; Thomsen, M.; Bolwig, T. G.; Knitowski, K. M.; McKinzie, D. L.; Yamada, M.; Wess, J.; Basile, A. *J. Neurosci. Res.* **2003**, *74*, 91.
13. Thomsen, M.; Woldbye, D. P.; Wortwein, G.; Fink-Jensen, A.; Wess, J.; Caine, S. B. *J. Neurosci.* **2005**, *25*, 8141.
14. Anney, R. J. L.; Lotfi-Miri, M.; Olsson, C. A.; Reid, S. C.; Hemphill, S. A.; Patton, G. C. *BMC Genet.* **2007**, *8*, 46.
15. Bridges, T. M.; Marlo, J. E.; Niswender, C. M.; Jones, J. K.; Jadhav, S. B.; Gentry, P. R.; Weaver, C. D.; Conn, P. J.; Lindsley, C. W. *J. Med. Chem.* **2009**, *52*, 3445.
16. Bridges, T. M.; Kennedy, J. P.; Hopkins, C. R.; Conn, P. J.; Lindsley, C. W. *Bioorg. Med. Chem. Lett.* **2010**, *20*, 5617.
17. Gentry, P. R.; Bridges, T. M.; Lamsal, A.; Vinson, P. N.; Smith, E.; Chase, P.; Hodder, P. S.; Engers, J. L.; Niswender, C. M.; Daniels, J. S.; Conn, P. J.; Wood, M. R.; Lindsley, C. W. *Bioorg. Med. Chem. Lett.* **2013**, *23*, 2996.
18. Gentry, P. R.; Kokubo, M.; Bridges, T. M.; Byun, N.; Cho, H. P.; Smith, E.; Hodder, P. S.; Niswender, C. M.; Daniels, J. S.; Conn, P. J.; Lindsley, C. W.; Wood, M. R. *J. Med. Chem.* **2014**, *57*, 7804.
19. Gentry, P. R.; Kokubo, M.; Bridges, T. M.; Cho, H. P.; Smith, E.; Chase, P.; Hodder, P. S.; Utley, T. J.; Rajapakse, A.; Byers, F.; Niswender, C. M.; Morrison, R. D.; Daniels, J. S.; Wood, M. R.; Conn, P. J.; Lindsley, C. W. *ChemMedChem* **2014**, *9*, 1677.
20. Gentry, P. R.; Kokubo, M.; Bridges, T. M.; Kett, N. R.; Harp, J. M.; Cho, H. P.; Smith, E.; Chase, P.; Hodder, P. S.; Niswender, C. M.; Daniels, S. J.; Conn, P. J.; Wood, M. R.; Lindsley, C. W. *J. Med. Chem.* **2013**, *56*, 9351.
21. Synthesis of VU6000181. To a suspension of Mg (936 mg, 38.5 mmol) and iodine (5 mg) in THF (2 mL) was added a part of a solution of 4-bromo-2-methylanisole (7.39 g, 36.8 mmol) in THF (9 mL) at ambient temperature. After initiating the reaction, a solution of 4-bromo-2-methylanisole diluted with THF (19 mL) was added dropwise to the mixture diluted with THF (10 mL). After the mixture was allowed to stir at ambient temperature for 2 h, resulting Grignard reagent was added to a suspension of phthalic anhydride **8** (5.18 g, 35.0 mmol) in THF (50 mL) at −65 °C. The mixture was allowed to stir for 2.5 h as temperature was elevated up to 0 °C. The reaction was quenched with cold water and the aqueous layer was separated. The organic layer was extracted with 1 N NaOH aqueous solution and the combined aqueous layer was acidified with 2 N HCl solution. The aqueous layer was extracted with ethyl acetate twice and the combined organic layer was washed with brine and dried over magnesium sulfate. The filtrate was evaporated under reduced pressure. The residue was triturated with ethyl acetate/diethyl ether to give compound **3** as a white powder (5.61 g, 59% yield). To a solution of compound **3** (1.0 g, 3.7 mmol) and *para*-toluene sulfonic acid monohydrate (10 mg) in PhMe (8 mL) and 1,4-dioxane (8 mL) was added ethylenediamine (0.50 mL, 7.4 mmol) at ambient temperature. The resulting white suspension was subjected to microwave irradiation at 150 °C for 30 min. After removing insoluble material, the filtrate was concentrated. The procedure above was repeated twice more and the three portions were combined and purified on silica gel using hexane/ethyl acetate as an eluent. Crude product was triturated with diethyl ether to give compound **4** as an off-white powder (1.69 g, 52% yield). To a solution of compound **4** (500 mg, 1.70 mmol) in dichloromethane (8 mL) was added DIPEA (0.74 mL, 4.25 mmol) and 3,4,5-trifluorobenzoyl chloride (0.33 mL, 2.55 mmol) at ambient temperature. After stirring for 30 min, cold $NaHCO_3$-aq was added to the mixture which was extracted with dichloromethane twice. The combined organic layer was concentrated under reduced pressure and the residue was purified on silica gel using hexane/ethyl acetate as an eluent. Crude product was triturated with diethyl ether/hexane to yield compound **7B-6** as a white powder (491 mg, 64% yield). Chiral resolution by SFC (Agilent 1260, Column: LUX cellulose-3, Column dimensions: 10 × 250 mm, Co-solvent: MeOH, Modifier: none, Gradient Profile: 10% isocratic, Flow Rate: 15 mL/min, Backpressure: 100, Column temperature: 40 degrees, retention time: 2.814 min, dated on July 30th) followed by concentration afforded **(*S*)-7B-6** (**VU6000181**) as a white powder. ^{1}H NMR (400.1 MHz, DMSO-d_6): 7.89 (d, *J* = 7.4 Hz, 1H), 7.80-7.78 (m, 1H), 7.71–7.57 (m, 4H), 7.03 (dd, *J* = 8.5, 2.5 Hz, 1H), 6.91 (d, *J* = 8.5 Hz, 1H), 6.86 (d, *J* = 2.5 Hz, 1H), 4.11–3.99 (m, 2H), 3.84–3.80 (m, 4H), 3.22–3.15 (m, 1H). ^{13}C NMR (100.6 MHz, DMSO-d_6):171.88, 165.56, 158.26, 150.99 (dd, *J* = 249, 9.8 Hz), 147.01, 140.76 (dt, *J* = 252, 15.6 Hz), 133.87, 133.68 (q, *J* = 6.1 Hz), 132.84, 131.18, 130.35, 129.48, 128.74, 126.61, 125.75, 124.18, 113.29 (dd, *J* = 16.5, 6.0 Hz), 110.94, 87.66, 56.25, 52.45, 40.24, 17.11. HRMS calcd for: $C_{25}H_{19}F_3N_2O_3$ (M+H), 425.1348; found 452.1352. Specific rotation $[\alpha]_D^{23}$ −169° (*c* = 0.75, $CHCl_3$).
22. Lavieri, R.; Scott, S. A.; Selvy, P. E.; Brown, H. A.; Lindsley, C. W. *J. Med. Chem.* **2010**, *53*, 6706.
23. Kennedy, J. P.; Williams, L.; Bridges, T. M.; Daniels, R. N.; Weaver, D.; Lindsley, C. W. *J. Comb. Chem.* **2008**, *10*, 345.
24. Zhao, Z.; Wisnoski, D. D.; O'Brien, J. A.; Lemiare, W.; Williams, D. L., Jr.; Jacobson, M. A.; Wittman, M.; Ha, S.; Schaffhauser, H.; Sur, C.; Pettibone, D. J.; Duggan, M. E.; Conn, P. J.; Hartman, G. D.; Lindsley, C. W. *Bioorg. Med. Chem. Lett.* **2007**, *17*, 1386.
25. Wenthur, C. J.; Niswender, C. M.; Morrison, R.; Daniels, J. S.; Conn, P. J.; Lindsley, C. W. *J. Med. Chem.* **2013**, *56*, 5208.
26. Mico, B. A.; Federowicz, D. A.; Ripple, M. G.; Kerns, W. *Biochem. Pharmacol.* **1988**, *37*, 2515.